Journal of Applied Polymer Science

Poly(lactic acid) biocomposites reinforced with ultrafine bamboo-char: Morphology, mechanical, thermal, and water absorption properties

Shaoping Qian,[1] Kuichuan Sheng,[1] Wenchao Yao,[1] Hui Yu[2]
[1]College of Biosystems Engineering and Food Science, Zhejiang University, Hangzhou 310058, China
[2]China National Research Center of Bamboo, Hangzhou 310012, China
Correspondence to: K. Sheng (kcsheng@zju.edu.cn)

ABSTRACT: In this study, ultrafine bamboo-char (BC) was introduced into poly(lactic acid) (PLA) matrix to improve mechanical and thermal properties of PLA based biodegradable composites. PLA/BC biocomposites were fabricated with different BC contents by weight. Uniform dispersion of BC in the PLA matrix and good interaction *via* physical and chemical interfacial interlocks were achieved. The maximum tensile strength and tensile modulus values of 14.03 MPa and 557.74 MPa were obtained when 30% BC was used. Impact strength of the biocomposite with 30% BC was increased by 160%, compared to that of pure PLA. DSC analysis illustrated that PLA/BC biocomposites had a better thermal property. Crystallization temperature decreased and maximal crystallinity of 30.30% was observed with 30% BC load. We did not notice significant thermal degradation differences between biocomposites with different BC loadings from TGA. Better water resistance was obtained with the addition of BC. © 2016 Wiley Periodicals, Inc. J. Appl. Polym. Sci. **2016**, *133*, 43425.

KEYWORDS: biopolymers and renewable polymers; blends; composites; differential scanning calorimetry (DSC); thermal properties

Received 28 September 2015; accepted 7 January 2016
DOI: 10.1002/app.43425

INTRODUCTION

Bamboo-char (BC), with extensive sources, inexpensive price, reasonable manufacturing cost, and unique properties, is a residual solid after pyrolysis of bamboo in a deficient atmosphere.[1] Besides the utilization in energy field, BC also has application potential in biocomposites due to its absorbability, abrasiveness, light absorbability, thermal insulation, and stability.[2,3] Moreover, bamboo grows abundantly in many tropical and subtropical regions in the world, especially in Asia, and is widely used in furniture manufacturing. However, abundant bamboo processing residuals cannot be effectively utilized. Carbonization is probably the most promising way to promote utilization value of bamboo residues. The ultrafine BC can be introduced into polymer biocomposites as reinforcement. In the previous literatures, bamboo-char were incorporated with poly(-olefins)[4] or PET/PP[5] matrix for functional optimization. Many properties such as tensile, water absorption, electrical resistance, electromagnetic shielding effectiveness, far-infrared ray radiativity were remarkably changed with the addition of bamboo-char.

Poly(lactic acid) (PLA), a biobased and biodegradable polymer, is usually made through ring-opening polymerization of lactide. Under the degradation of bacteria, acid and/or alkali, etc., the final degradation products of PLA are H_2O and CO_2.[6,7] In the past decades, PLA drew much attention as one of most potential materials that could be used to replace the traditional petroleum-based plastics since it was green and pollution-free. Currently, PLA is applied in many fields such as biomedicine, textile, film, decorative panel, electrical element, and food package.[8–10] However, due to its poor crystallization property, the thermal and mechanical properties of PLA have been gradually compromised and it presents low thermal stability and high brittleness,[11] which restricts the extensive industrial application. Therefore, it is necessary to develop approaches to improve PLA properties.

Improving the crystallization property of PLA is an effective approach to increase the mechanical and thermal properties. Relevant researches indicated that introducing of inorganic fillers (e.g., montmorillonite, kaolinite, talcum powder, hydroxyapatite, silicon dioxide, titanium dioxide, carbon nanotube, carbon black, magnesium oxide, zinc oxide, etc.) into PLA matrix enhanced the crystallization behavior by heterogeneous nucleation and/or plasticization. As a result, the thermal and mechanical properties of composites were improved.[12–17] Zhang *et al.* adopted solution casting method to prepare composites made from 325-mesh alkylated graphene and PLA. Results showed that the graphene was evenly dispersed in the substrate and the crystallization capacity and mechanical strength were significantly improved.[18] Zhao *et al.* conducted carboxyl grouping treatment of multiwalled

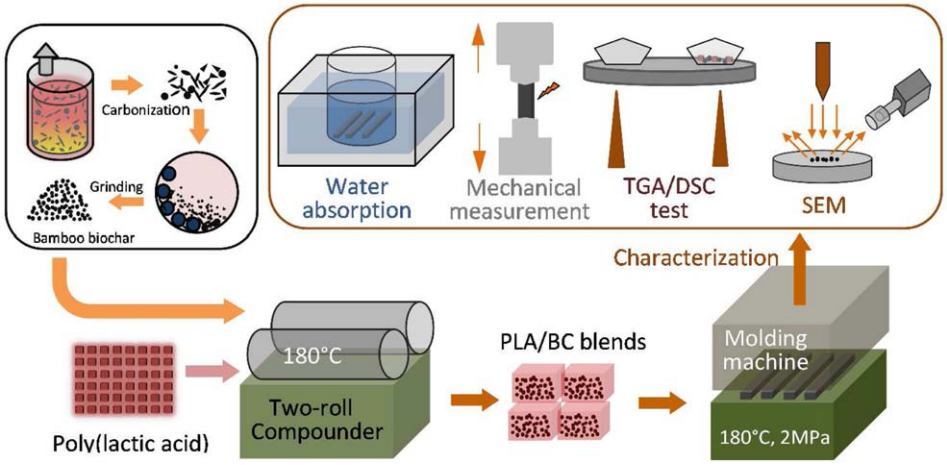

Figure 1. Preparation and characterization of the biocomposites. [Color figure can be viewed in the online issue, which is available at wileyonlinelibrary.com.]

carbon nanotubes and then employed solution mixing technique to prepare PLA/carbon nanotubes biocomposites.[19] They reported that the nanotubes improved the crystallization property of PLA. Liu *et al.* summarized the influence of PLA molecular crystalline forms on the property of biocomposites and reviewed the promoting effect of fillers on crystallization property of PLA.[20] Ho *et al.* conducted the comparison on tensile, flexural and impact properties of bamboo-char particle reinforced PLA composites with the content ranging from 2.5 to 10 wt %.[21] Wang *et al.* studied the influence of carbon black on the properties of plasticized poly(lactic acid) composites and revealed the enhancement of carbon black in PLA matrix.[15] However, there has been barely studies reporting the wide content range of BC (up to 40 wt %) enhancing PLA composite and its microstructure, interfacial interaction and macroproperties remain unclear.

In this article, ultrafine BC particles of different loadings range of 0–40%(w/w) were added as fillers to fabricate PLA/BC biocomposites. Scanning electron microscope (SEM) and Fourier transform infrared spectroscopy (FT-IR) were employed to analyze the morphology and interfacial bonding of the biocomposites. Differential scanning calorimetry (DSC) and thermal gravity analysis (TGA) were utilized to investigate the crystallization and thermal property of the biocomposites. Water absorption, mechanical property and micro-structure of the biocomposites were characterized. Finally, the optimal loading proportion of BC was obtained, thus providing basic data for further properties improvement and application expanding of PLA biocomposites. Their most likely application would be as reinforcing agent in structural material for green packaging composites replacing non-degradable plastic.

EXPERIMENTAL

Materials

Ultrafine BC (1000 mesh) was kindly provided by Tonfus Agri-biomass Sci. (Hangzhou, China). BC particle size was determined by using Mastersizer 2000 (Malvern Instruments, England). According to the tested results, the average particle size of BC was 9.52 μm, and 90 wt % of the BC was smaller than 26.5 μm. PLA pellets (ES701, melt index 10.8 g/10 min at 190 °C, T_g 54.6 °C and T_m 149.7 °C) were obtained from Tongjieliang Biomaterials (Shanghai, China). Potassium bromide (KBr) was purchased from Aladdin (Shanghai, China).

Preparation of PLA/BC Biocomposites

BC to PLA ratios were set to 0, 5, 10, 15, 20, 25, 30, 35, and 40% by weight. The blends were prepared in a double roll lab-scale compounder under the conditions of 180 °C and 50 rpm for 20 min. Closed mould hot compressing technique was used to fabricate PLA/BC biocomposites. The mould was exactly the size of specimens. The equipment used and procedures could be referred in our article concerning PLA/bamboo particles composites preparation.[22] The size of samples for tensile and impact tests were 165 × 13 × 4 mm^3 and 100 × 10 × 4 mm^3, respectively, on the basis of ASTM D 638 and ASTM D 6110. All samples were kept in desiccator for further characterization (see Figure 1).

Surface Morphology Observation

Surface morphology of BC, fractured surface, before and after water absorption of PLA/BC biocomposites was observed using scanning electron microscope (SU8010, Hitachi, Japan). The samples were coated with gold before observing. The launching voltage of electron microscope was 10.0 kV.

Fourier Transform Infrared Spectroscopy (FT-IR)

FT-IR (Nicolet-380, Thermofisher Scientific) was adopted for infrared representation with the scanning range of 4000–400 cm^{-1}. The spectra were obtained with the KBr pellet technique. BC, PLA, and 30% loading PLA/BC biocomposites were ground into powder, then mixed and compressed with KBr powder into thin discs. 16 scans were co-added.

Mechanical Properties

Tensile test of PLA/BC biocomposites was carried out by using universal testing machine (CMT4503, MTS Inc.) according to ASTM D638, the gauge length and the crosshead speed for tensile test were set to 50 mm and 5 mm min^{-1}, respectively. Charpy impact test was conducted by a pendulum impact testing machine (ZBC 1251-B, MTS) according to ASTM D 6110. Samples were unnotched. Five specimens were used for each test.

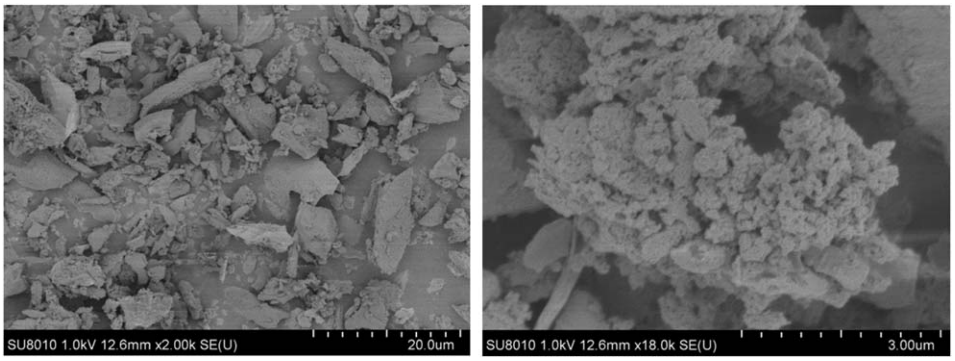

Figure 2. SEM micrographs of pure BC.

Differential Scanning Calorimetry (DSC)

DSC (200F3, Netzsch) was adopted to study the thermal properties of pure PLA and the biocomposites. About 10.0 mg sample was weighed and hermetically sealed. The samples were heated from the room temperature to 180 °C at a rate of 20 °C min^{-1}, kept for 3 min, then cooled down to 0 °C at a rate of 15 °C min^{-1}, and then heated again to 180 °C at a rate of 10 °C min^{-1}. The second DSC thermograms were recorded for further evaluation. Nitrogen was used as purging gas at a rate of 50 mL min^{-1}. An empty aluminium pan was used as reference. Crystallinity (X_c) was estimated according to the following equation,

$$X_c(\%) = \frac{\Delta H_c}{\Delta H_0 \times X_{\mathrm{PLA}}} \times 100\% \quad (1)$$

where ΔH_c refers to the crystallization enthalpy of PLA/BC biocomposites; ΔH_0 refers to the enthalpy value during 100% crystallization of PLA, which is 93.6 J g^{-1};[23] X_{PLA} refers to the weight ratio of PLA in PLA/BC biocomposites.

Thermogravimetric Analysis (TGA)

Thermal stability of PLA/BC biocomposites were determined by thermo-gravimetric analyzer (STA 409C, Netzsch). For this, about 10 mg of sample was taken in a standard ceramic crucible and heated from 30 to 600 °C at heating rate of 15 °C min^{-1} under a nitrogen flow of 50 mL min^{-1}. An empty crucible was used as a reference.

Water Absorption

Water absorption was evaluated according to the ASTM D 570-98 standard.[24] The dimensions of the specimens were 100 × 10 × 4 mm^3. Three specimens of each sample were dried in an oven at 45 °C for about 24 h (weight: m_0), then submerged in distilled water at 100 °C. Periodically, each specimen was taken from the water and subsequently weighed after its surface moisture was carefully removed with an absorbent paper and weighed (weight: m_t). For each increment of time, water absorption rate (M_t) of specimens was calculated as a percentage of initial weight.

In the literature Fick analytical models presented in eq. (2) are proposed to describe the diffusion kinetic of PLA-matrix biocomposites systems.[25] The ability of water penetration into composites can be evaluated by analysis of the diffusion coefficient D [eq. (3)].[26]

$$\log\left(\frac{M_t}{M_S}\right) = \log(k) - n\log(t) \quad (2)$$

$$\frac{M_t}{M_S} = \frac{4}{L}\left(\frac{D}{\pi} \times t\right)^{0.5} \quad (3)$$

where M_t refers to the moisture content at time t and M_S corresponds to the moisture content at equilibrium. When the $\log(M_t/M_S)$ was plotted as a function of time, the linear part of the obtained curve could be used to determine the linear coefficient "k." L is the thickness of the sample.

RESULTS AND DISCUSSION

Micromorphology Analysis

Figure 2 indicates surface morphology of BC particles in terms of size, aspect, and topography. The shapes of BC were irregular and seem to encompass mainly two populations. As for one type, the particle size and aspect ratio were relatively large, the surface was flat with fewer pore and texture, and the length size was 10–20 μm, while the other included a relatively small (1–5 μm) particle size with rough surface, developed pores, similar to activated charcoal. The characteristics of the two population of BC were similar to that of olive stone flour reported by Naghmouchi *et al.*[27] The difference of two populations might be the consequence of the carbonization of two substances, namely, bamboo fiber and parenchymatous tissue. These pores could generate relatively strong capillary effect.[28,29] As a result, the infiltration effect of PLA matrix was improved so as to enhance the interfacial interaction between the two phases.

FT-IR Analysis

FT-IR spectra of pure PLA, BC and biocomposites with 30% BC are shown in Figure 3. A relatively strong hydroxyl (—OH) stretching vibration peak appeared in BC around 3426 cm^{-1}, which resulted from the abundant hydroxyls in BC particle molecules. Besides, carboxyl with C=O bond (1694 cm^{-1}), quinone (1650 cm^{-1}) and aromatic C=C bond (1600 cm^{-1}) were also observed.[30] Strong absorption also existed in the range from 1100 to 1000 cm^{-1}, which was mainly resulted from SiO_2 (1030 cm^{-1}) in ash formed during the pyrolysis. FT-IR spectra of biocomposites were basically consistent with that of PLA and no transfer of absorption peak took place, which indicated that there were physical interlocks between two phases. As we know, both BC and PLA are hydrophobic, so the phases would present a good surface compatibility. However, the connection mostly maintained by Van der Waals' force and hydrogen-bond interaction, which is relatively

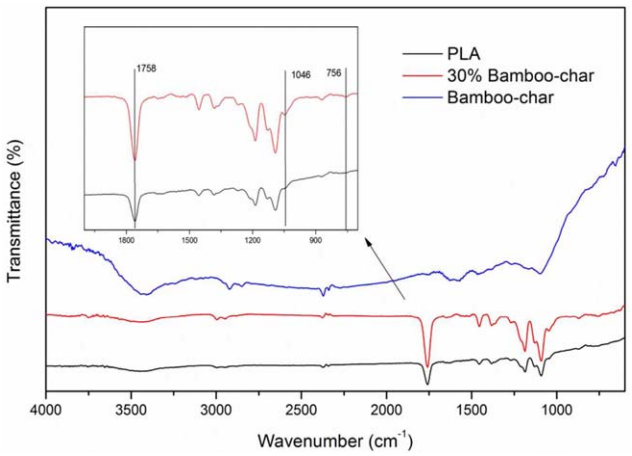

Figure 3. FT-IR spectra of pure PLA, BC and PLA/BC biocomposites added with 30% of BC. [Color figure can be viewed in the online issue, which is available at wileyonlinelibrary.com.]

low. However, the peaks of carbonyl (—C═O) stretching vibration (1758 cm^{-1}) and hydroxyl bending (1046 cm^{-1}) were strengthened, which probably suggested the chemical bonding between PLA molecule and BC after compounding. Moreover, out-of-plane vibration absorption peak of C—H on benzene ring was generated at 756 cm^{-1}. Consequently, both physical connection and chemical bonds existed between two phase interfaces of PLA and BC.

Mechanical Properties of PLA/BC Biocomposites

As shown in Figure 4, tensile modulus increased linearly along with the increase of BC content from 5 to 30%, which was related to the characteristics of the incorporated filler and less affected by the polymer–filler adhesion since the stiffness of BC particles was much higher than that of PLA. Many models could be simulated the Young's modulus, and Hirsch model was a common one.[31] It combined parallel and series rule of mixture models and presented quite accuracy during prediction of elasticity modulus of composites with randomly distributed particles. The fitting formula is shown in eq. (4):

$$E_t^c = \beta(E_t^P V^P + E_t^m(1-V^P)) + (1-\beta)\frac{E_t^P E_t^m}{E_t^m V^P + E_t^P(1-V^P)} \quad (4)$$

where β refers to stress transmission efficiency factor between particle and matrix; E_t refers to elasticity modulus and V refers to volume ratio, while c, m, and P refer to composites, matrix and particles, respectively. Based on the relevant literatures, β was determined as 0.4 for short lignocellulosic fibers correctly fit the experimental data.[27] Adopting the Hirsh model, and a β value equal to 0.4, higher correlation of the intrinsic Young's modulus of BC prediction in this loading interval could be obtained by adjusting elasticity modulus E^P. The intrinsic Young's modulus of BC was estimated to 50.6–120.3 GPa.

Tensile strength, tensile modulus, and elongation at break were relative lower than those of pure PLA when BC was added into PLA initially. This phenomenon was similar to that reported by

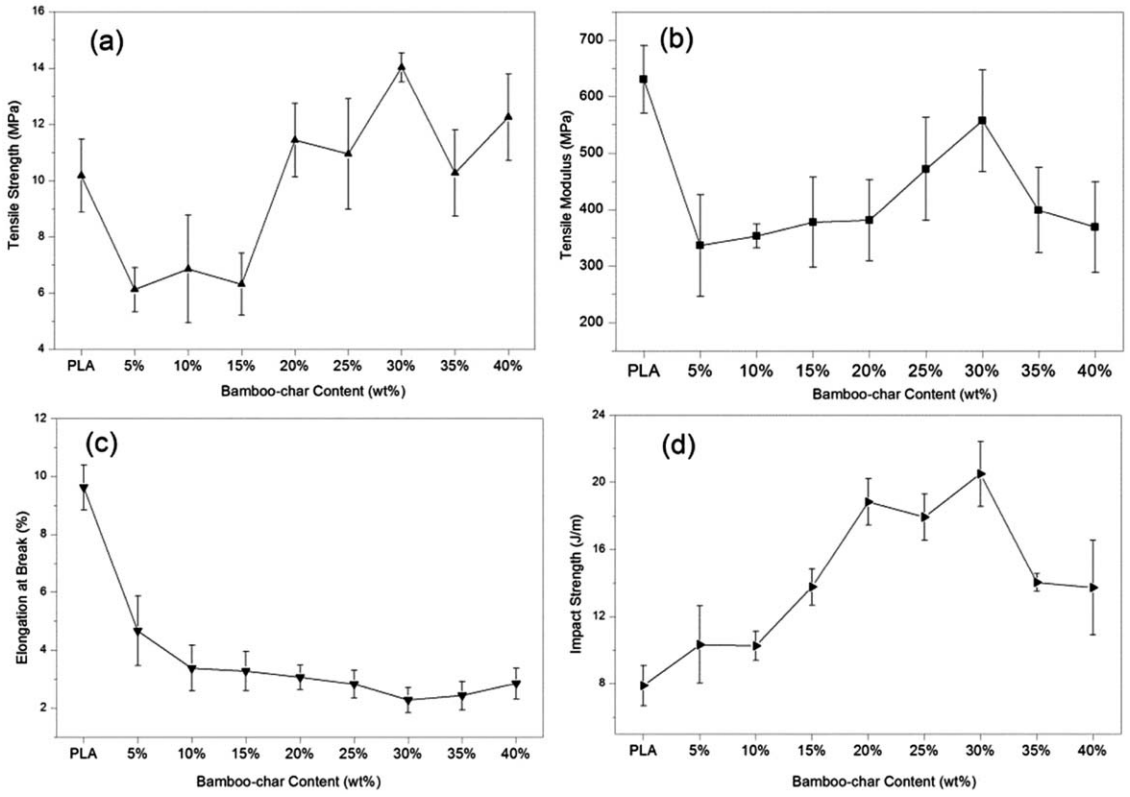

Figure 4. Mechanical property of pure PLA and PLA/BC biocomposites, (a) tensile strength; (b) tensile modulus; (c) elongation at break; (d) impact strength.

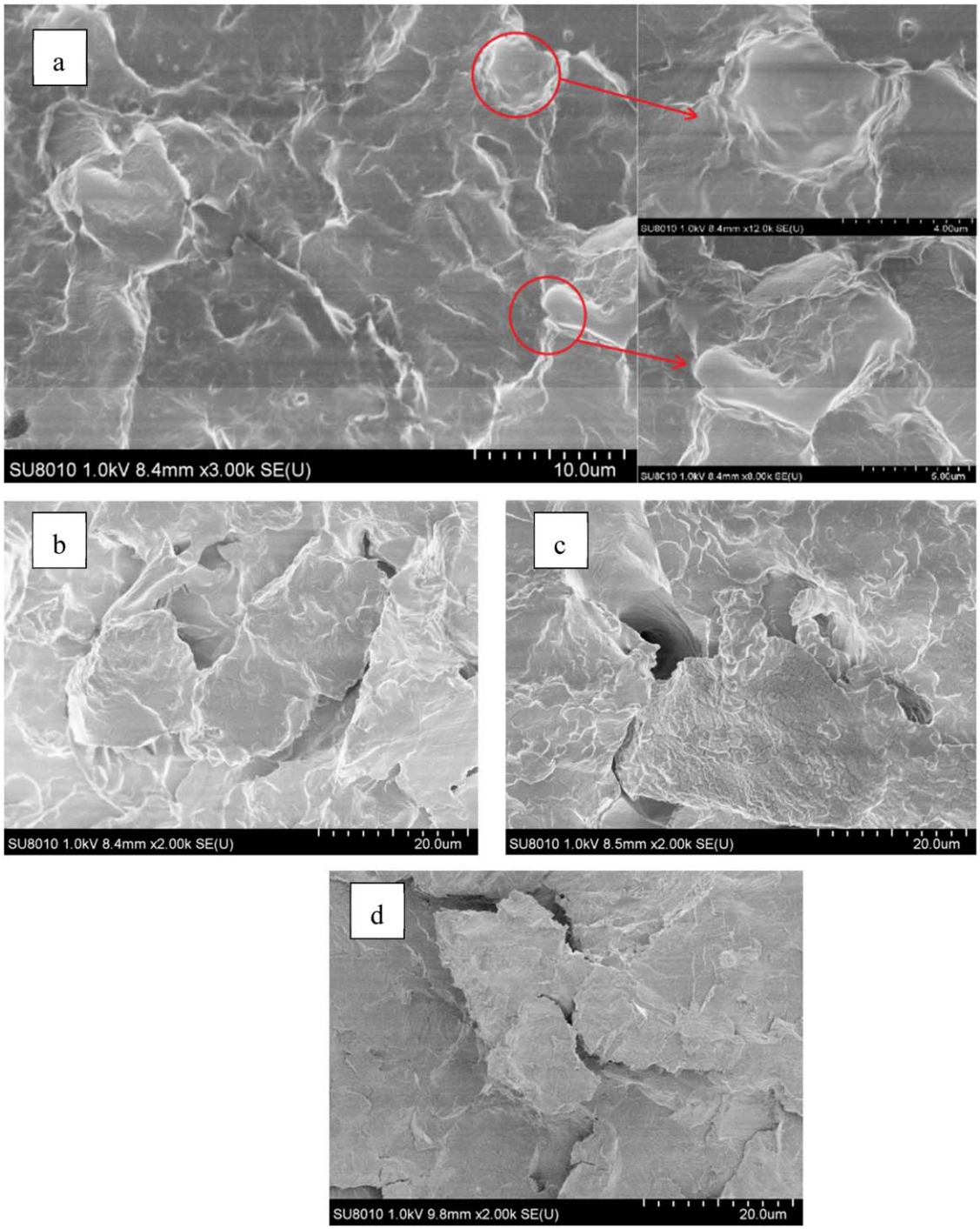

Figure 5. SEM micrograph of the tensile fractured surface for PLA/BC biocomposites, (a) 30%; (b) 5%; (c) 10%; (d) pure PLA. [Color figure can be viewed in the online issue, which is available at wileyonlinelibrary.com.]

other researchers. It was resulted from the lack of efficient interfacial bonding between filler and matrix.[32] However, with increase of BC loading, tensile strength and modulus both increased and reached the maximal values of 14.03–557.74 MPa, respectively, when the BC loading was 30%, which was higher than that of LDPE/bamboo-char composites.[5] After that, both decreased slightly with a further increasing of BC content. Different from extremely hydrophobic matrix like PP and PE reinforced with lignocellulosic filler (without coupling reagent), from which steady drop in strength observed.[33] This behavior might be due to the increased degree of crystallinity of biocomposites with BC additions, leading to more regularized molecular chain of PLA. Abundant BC particles were placed in lattice to continually enhance the tensile strength and modulus of the biocomposites. Even more, the tensile strength of biocomposites with 30% loading of BC was greater than that of pure PLA. Elongation at break

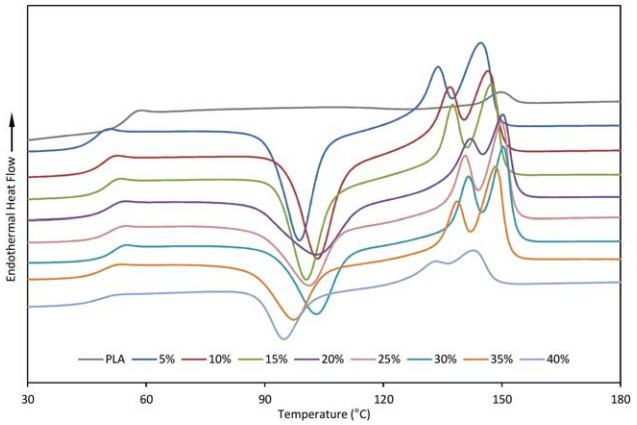

Figure 6. DSC behaviors of pure PLA and PLA/BC biocomposites. [Color figure can be viewed in the online issue, which is available at wileyonlinelibrary.com.]

continuously decreased with the increase of BC loadings. However, the decrease of elongation at break became non-significant after loading exceed 10%. This tendency mainly resulted from the low aspect ratio of BC because of stress concentration during tensile deformation and breakage. Indeed, in particle or fiber biocomposites, despite great importance of interfacial bonding between matrix and filler, proper size of filler was still required in order to transfer the stress from matrix to filler.[34] The characteristics of interface bonding of BC filler and PLA matrix after tensile fractured are shown in Figure 5. As shown in Figure 5(a), when BC loading was 30%, BC was favorably dispersed in PLA matrix. Pores of BC were covered by PLA, indicating the enhanced physical and chemical bonding between BC and polymer matrix in comparison to those with 5% [Figure 5(b)] and 10% [Figure 5(c)] loads. Meanwhile, PLA film on the BC was ordered and smooth, indicating better molecular chain array orientation, leading to high degree of crystallinity and strong bonding force. And the stress dispersion was relatively uniform during tension test. Figure 5(b,c) illustrated the uneven distribution and air bubbles in the biocomposites when BC loadings were 5 and 10%, which was likely the consequence of the over active plasticization. Figure 5(d) showed the fracture surface of pure PLA, which was relatively smooth. As a result, the fluidity of PLA increased, PLA molecular chain was difficult to adhere to the particles. Stress concentration could be easily caused, resulting in drop of tensile property. So the

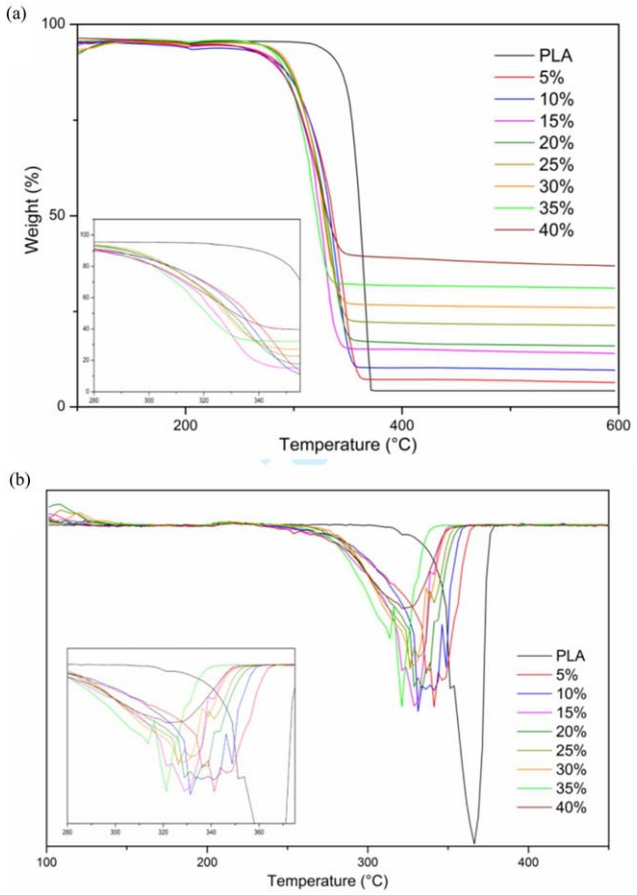

Figure 7. TGA and DTG of PLA and biocomposites with different BC loading, (a) TGA; (b) DTG. [Color figure can be viewed in the online issue, which is available at wileyonlinelibrary.com.]

tensile property of composites with 30% BC was better compared to that of 10% BC.

As shown in Figure 4(d), with the increase of BC loading, impact strength was largely increased and reached a maximum value of 20.50 J m^{-1} when the loading reached 30%, improved by 160% compared with pure PLA of 7.88 J m^{-1}. Similar findings were reported by Ho *et al.* that the total fracture energy of pure PLA were increased from 1.80 to 2.69 J of 7.5 wt % BC/PLA.[21] It was

Table I. DSC Data of PLA and PLA/BC Biocomposites

Samples	T_g (°C)	T_{cc} (°C)	ΔH_c (J g^{-1})	X_c (%)	T_{m1} (°C)	T_{m2} (°C)	ΔH_m (J g^{-1})
PLA	54.6	126.3	2.93	1.09	None	149.7	2.083
5%	46.4	98.5	25.38	28.54	133.6	144.4	28.39
10%	48.3	103	24.56	29.16	136.6	146.2	28.82
15%	49.6	100.1	23.12	29.06	137.2	146.9	23.62
20%	50.4	102.9	22.29	29.77	139.7	148.9	24.44
25%	50.8	101.3	20.64	29.40	140.2	149.2	23.99
30%	51.2	102.7	19.85	30.30	141.2	150.0	23.29
35%	49.1	96.9	15.68	25.77	138.3	148.0	22.96
40%	48.1	94.4	11.47	22.06	133.1	142.4	13.77

Table II. TGA Data of PLA/BC Biocomposites

Samples	T_{onset} (°C)	Temp. range (°C)	T_{max} (°C)	Mass loss (%)
PLA	314.2	314.2-354.9	365.9	92.92
5%	314.2	314.2-354.9	343.5	82.23
10%	312.5	312.5-352.9	330.7	78.61
15%	306.1	306.1-339.2	329.7	77.79
20%	307.0	307.0-347.6	328.1	74.26
25%	310.1	310.1-338.9	326.5	66.30
30%	311.6	311.6-334.6	324.1	64.78
35%	307.9	307.9-321.5	314.8	57.43
40%	291.7	291.7-328.8	312.5	53.12

because that PLA was a semicrystalline polymer with relatively low degree of crystallinity and poor molecular chain orientation so as to the impact resistance of molecular chain segment was relatively weak when the polymer was impacted. With the addition of BC, the crystallization of biocomposites was significantly enhanced, and the molecular chain was self-arranged in a regular way to form a large crystalline region, thus enhancing resistance against generation of incipient crack. Additionally, since the favorable interfacial bonding between BC and PLA, part of energy was dispersed through filler–matrix interfacial debonding to obstruct the propagation of crack once the crack was initiated. When addition amount exceeded 30%, excessive rigid BC particles caused stress concentration to reduce incipient energy of crack and resulted in early interfacial debonding between matrix and filler so as to cause decrease of impact strength.[28]

Thermal Properties of PLA/BC Biocomposites

DSC curves of pure PLA and PLA/BC biocomposites with different loadings are shown in Figure 6. Table I tabulated the thermal parameters including glass transition temperature (T_g), cold crystallization temperature (T_{cc}), crystallization enthalpy (ΔH_c), degree of crystallinity (X_c) and melting temperature (T_m). With the increase of BC loading, T_g increased first and then decreased.

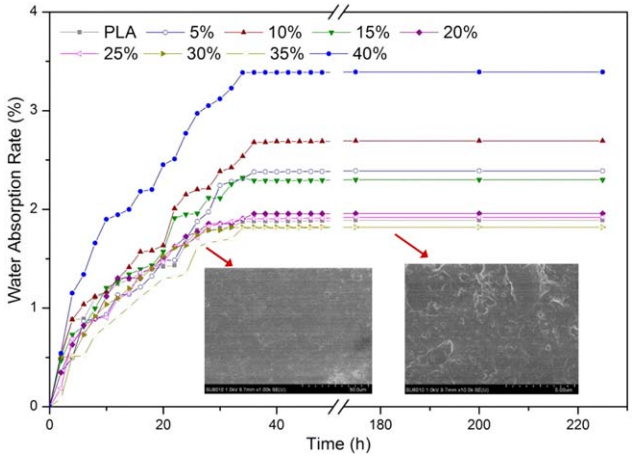

Figure 8. Water absorption rate vs. time of the biocomposites. [Color figure can be viewed in the online issue, which is available at wileyonlinelibrary.com.]

Table III. Kinetic Constants of PLA/BC Biocomposites

Samples	Log k	k	n	r^2
PLA	−1.4067	0.0392	−0.4982	0.9889
5%	−1.2111	0.0615	−0.4265	0.9896
10%	−1.1945	0.0639	−0.4582	0.9699
15%	−1.2204	0.0602	−0.3887	0.9625
20%	−1.2832	0.0521	−0.4394	0.9862
25%	−1.2725	0.0534	−0.5233	0.9857
30%	−1.4191	0.0381	−0.5851	0.9782
35%	−1.3990	0.0399	−0.3769	0.9559
40%	−1.1811	0.0659	−0.4562	0.9517

It was probably because that plasticization improved the mobility of PLA molecular chain with the addition of BC. When the content of BC reached 30%, a higher value of 51.2 °C was obtained but it was still lower than pure PLA. It was because the heterogeneous nucleation restricted the mobility of PLA molecular chain. Similar results was noticed by Ho *et al.* and Su *et al.*, which was attributed to the less requirement of energy for its molecule movement.[21,35] T_{cc} and X_c changed significantly after addition of BC. T_{cc} decreased by 31.9 °C and X_c improved by 29.21% at most, which may be attributed to the fact that BC acted as nucleating agents in PLA matrix. Su *et al.* also reported carbon black facilitated the crystallization rate and had higher crystallization peak temperature using WAXD, SAXS and DSC analysis.[36] Consequently, capacity of formation of crystal nucleus and growing ability of crystal nucleus were substantially improved under the effect of heterogeneous nucleation so as to significantly promote X_c. Double crystallization melting peaks are observed in PLA/BC biocomposites, whereas the pure PLA presents single (Figure 6). It was probably because that the peak at the lower temperature was related to the melting of the α' form crystal and its recrystallization into the α form, while the second peak corresponded to the melting of the α form crystal. The melting of the α' form and the recrystallization into the α form could be considered as the α'–α phase transition.[37] In addition, with the increase of BC loading, the melting temperature increased first and then deceased, and a higher value was also obtained when the loading was 30%. It could be deduced that the crystallization capacity of biocomposites remarkably improved and cold crystallization was incomplete under a certain heating rate. As a result, the incomplete crystal at low melting temperature was re-crystallized to form a relatively complete crystal and then generated a high temperature melting peak. With the addition of BC, the crystallization behavior of biocomposites gradually increased and the thermal stability was enhanced. Conversely, when loading content exceeded 30%, excessive BC hindered lateral rearrangements of PLA chains and crystallization of PLA films.

Thermal Stability of PLA/BC Biocomposites

Figure 7(a,b) describe TGA and DTA curves of pure PLA and biocomposites with different BC loadings. Table II listed thermogravimetric analysis parameters including starting temperature (T_{onset}), temperature range of thermal degradation, maximum temperature of thermal degradation rate (T_{max}) and mass loss

rate. All samples presented single thermal degradation stage, but ranges of degradation temperature and T_{max} were slightly different. With the increase of BC, these three parameters decreased slightly. Pure PLA, however, presented relatively high thermal stability. It might be because that pure PLA absorbed more heat to cause the breakage of a relatively long molecular chain. When BC was added, the mobility of PLA molecular chain was enhanced and some long molecular chains were decomposed to form crystals due to plasticization and heterogeneous nucleation, resulting in the decrease of thermal degradation. This trend was similar to PLA/fiber composites reported by literatures.[38] T_{onset} firstdecreased and then increased, which indicated that the improvement of crystallization enhanced the thermal stability of the biocomposites. As to BC filler, it was the product of pyrolysis, and basically had no mass loss during thermal degradation. Therefore, the mass loss was relatively high when the BC loading was low.

Water Absorption

Figure 8 presents the water absorption curves of BC loadings reinforced PLA biocomposites. Biocomposites with 40% BC loading showed the highest equilibrium water absorption, while the loading of 30 and 35% had the lower water absorptions. Pure PLA, 20 and 25% loadings presented similar equilibrium water absorptions and were no significant difference with 30 and 35% loadings. These findings supported that the introducing proper of ultrafine BC into the PLA structure enhanced the water resistance. As seen in SEM observations, biocomposites with 30% BC showed a better combination between PLA matrix and fillers. Moreover, pores and cracks on the BC were permeated by PLA molecular, which led to improved water resistance.

Kinetic parametric constants of PLA/BC biocomposites obtained by diffusion analysis is listed in Table III. The linearity presented curves of $\log(M_t/M_S)$ vs. time $[\log(t)]$ are well fit with Fick's diffusion law. The parameter k is related to the affinity between the composite and water. The increase of BC loading affected a lot in the affinity between the biocomposites and water molecule due to the crystallization, and further preventing water uptake. Comparing to our previous study with bamboo particles reinforced polyvinyl chloride composites,[39] PLA/BC biocomposites showed lower moisture diffusivity. It probably because that both PLA and BC are hydrophobic materials.

The diffusion coefficient D is proportional to k according to eqs. (2) and (3). The higher the value of D, the quicker the diffusion of water molecules in the biocomposites.[25] The biocomposites with 5–15% loadings had relatively higher D value than those with 20–35% loadings, and the 40% loading got the highest D value. These findings are quite consistent with the water absorption curve. During the processing, we found that relatively low BC content in the PLA showed a plasticization function. However, the excessive plasticization caused by addition of BC hindered to form crystalline area, speeded up the water penetration, thus increasing the value of D. Furthermore, water resistance was notably enhanced when the loading was 30%. This could be due to the high crystallization with more dense and structured crystalline region, so that water molecular were difficult to permeate and diffusion in the biocomposites. In additon, the flowability of the blends become very low with 40% BC loading. The biocomposites showed the highest water absorption and D value, which is interpreted in terms of increasing of capillarity attraction attributed to an undercrosslinked at particle vicinity with excessive BC.

CONCLUSIONS

PLA biocomposites reinforced with 1000 mesh ultrafine bamboo-char were prepared. BC dispersed favorably in PLA matrix and the two phases had good interfacial interaction when BC content was 30%. Tensile strength and modulus increased with BC loadings increased from 5 to 30%, then slightly decreased. The maximum values of 14.03 MPa and 557.74 MPa were obtained at 30%, respectively. Impact strength was significantly increased and reached a maximal value of 20.50 J m^{-1} when BC load reached 30%. Elongation at break of biocomposites was lower than that of pure PLA. However, the decrease of elongation at break became nonsignificant after BC load exceeded 10%. The addition of BC lowered glass transition temperature and crystallization temperature and improved degree of crystallinity, melting temperature, and thermal stability of biocomposites. Different loadings of BC had no significant influence on thermal degradation stability of the biocomposites. Nearly 30% loading of BC improved the water resistance of the biocomposites. Finally, this work provides basic data for further improving the properties of PLA biocomposites and expanding the application of PLA biocomposites.

ACKNOWLEDGMENTS

The authors are grateful to the National Science & Technology Pillar Program of China (No. 2012BAC17B02) and the Forestry Scientific Cooperation Project between Zhejiang Province and Chinese Forestry Academy (No. 2013SY05) for financial support.

REFERENCES

1. Chen, D. Y.; Zhou, J. B.; Zhang, Q. S. *Bioresour. Technol.* **2014**, *169*, 313.
2. Gu, X. X.; Wang, Y. Z.; Lai, C.; Qiu, J. X.; Li, S.; Hou, Y. L.; Martens, W.; Mahmood, N.; Zhang, S. Q. *Nano Res.* **2015**, *8*, 129.
3. Xu, T.; Lou, L. P.; Luo, L.; Cao, R. K.; Duan, D. C.; Chen, Y. X. *Sci. Total Environ.* **2012**, *414*, 727.
4. Lin, J. H.; Lou, C. W.; Chen, J. M.; Hsieh, C. T.; Liu, Z. *Adv. Mater. Res.* **2008**, *5557*, 433.
5. Kittinaovarat, S.; Suthamnoi, W. *J. Met. Mater. Miner.* **2009**, *19*, 9.
6. Haafiz, M. K. M.; Hassan, A.; Zakaria, Z.; Inuwa, I. M.; Islam, M. S.; Jawaid, M. *Carbohydr. Polym.* **2013**, *98*, 139.
7. Hu, Y. M.; Wang, Q. L.; Tang, M. R. *Carbohydr. Polym.* **2013**, *96*, 384.
8. Franco-Urquiza, E. A.; Cailloux, J.; Santana, O.; Maspoch, M. L.; Infante, J. C. V. *Adv. Polym. Technol.* **2015**, *34*, 21470.
9. Shirai, M. A.; Grossmann, M. V. E.; Mali, S.; Yamashita, F.; Garcia, P. S.; Muller, C. M. O. *Carbohydr. Polym.* **2013**, *92*, 19.

10. Jariyasakoolroj, P.; Chirachanchai, S. *Carbohydr. Polym.* **2014**, *106*, 255.
11. Xiong, Z.; Li, C.; Ma, S. Q.; Feng, J. X.; Yang, Y.; Zhang, R. Y.; Zhu, J. *Carbohydr. Polym.* **2013**, *95*, 77.
12. Liu, Z. W.; Chou, H. C.; Chen, S. H.; Tsao, C. T.; Chuang, C. N.; Cheng, L. C.; Yang, C. H.; Wang, C. K.; Hsieh, K. H. *Polym. Compos.* **2014**, *35*, 1744.
13. Rizzi, S. C.; Heath, D. T.; Coombes, A. G. A.; Bock, N.; Textor, M.; Downes, S. *J. Biomed. Mater. Res.* **2001**, *55*, 475.
14. Wang, H. L.; Shu, L. P.; Jiang, S. T. *J. Appl. Polym. Sci.* **2010**, *117*, 2790.
15. Wang, N.; Zhang, X.; Ma, X.; Fang, J. *Polym. Degrad. Stabil.* **2008**, *93*, 1044.
16. Rhim, J. W.; Park, H. M.; Ha, C. S. *Prog. Polym. Sci.* **2013**, *38*, 1629.
17. Lahiri, D.; Rouzaud, F.; Namin, S.; Keshri, A. K.; Valdes, J. J.; Kos, L.; Tsoukias, N.; Agarwal, A. *ACS Appl. Mater. Interfaces* **2009**, *1*, 2470.
18. Pluta, M. *J. Polym. Sci. B: Polym. Phys.* **2006**, *44*, 3392.
19. Zhao, Y. Y.; Qiu, Z. B.; Yang, W. T. *Compos. Sci. Technol.* **2009**, *69*, 627.
20. Liu, G. M.; Zhang, X. Q.; Wang, D. J. *Adv. Mater.* **2014**, *26*, 6905.
21. Ho, M.; Lau, K.; Wang, H.; Hui, D. *Compos. Part B Eng.* **2015**, *81*, 14.
22. Qian, S. P.; Mao, H. L.; Sheng, K. C.; Lu, J.; Luo, Y. F.; Hou, C. Y. *J. Appl. Polym. Sci.* **2013**, *130*, 1667.
23. Li, Y.; Chen, C.; Li, J.; Sun, X. S. *J. Appl. Polym. Sci.* **2012**, *124*, 2968.
24. Srubar, W. V.; Frank, C. W.; Billington, S. L. *Polymer* **2012**, *53*, 2152.
25. Li, C.; Fan, H.; Wang, D. Y.; Hu, J.; Wan, J.; Li, B. *Compos. Sci. Technol.* **2013**, *87*, 189.
26. Nogueira, P.; Ramirez, C.; Torres, A.; Abad, M.; Cano, J.; Lopez, J.; López-Bueno, I.; Barral, L. *J. Appl. Polym. Sci.* **2001**, *80*, 71.
27. Naghmouchi, I.; Mutjé, P.; Boufi, S. *J. Appl. Polym. Sci.* **2014**, *131*, 41083.
28. Islam, M. S.; Pickering, K. L.; Foreman, N. J. *J. Appl. Polym. Sci.* **2011**, *119*, 3696.
29. Imre, B.; Keledi, G.; Renner, K.; Moczo, J.; Murariu, M.; Dubois, P.; Pukanszky, B. *Carbohydr. Polym.* **2012**, *89*, 759.
30. Ayana, B.; Suin, S.; Khatua, B. B. *Carbohydr. Polym.* **2014**, *110*, 430.
31. Espinach, F. X.; Julian, F.; Verdaguer, N.; Torres, L.; Pelach, M. A.; Vilaseca, F.; Mutjeb, P. *Compos. B Eng.* **2013**, *47*, 339.
32. Chinh, N. T.; Trang, N. T. T.; Thanh, D. T. M.; Hang, T. T. X.; Giang, N. V.; Quan, P. M.; Dung, N. T.; Hoang, T. *J. Appl. Polym. Sci.* **2015**, *132*, 41690.
33. Karnani, R.; Krishnan, M.; Narayan, R. *Polym. Eng. Sci.* **1997**, *37*, 476.
34. Abdelmouleh, M.; Boufi, S.; Belgacem, M. N.; Dufresne, A. *Compos. Sci. Technol.* **2007**, *67*, 1627.
35. Su, Z.; Huang, K.; Lin, M. *J. Macromol. Sci. B* **2012**, *51*, 1475.
36. Su, Z.; Liu, Y.; Guo, W.; Li, Q.; Wu, C. *J. Macromol. Sci. B* **2009**, *48*, 670.
37. Tabi, T.; Sajó, I.; Szabo, F.; Luyt, A.; Kovács, J. *Express Polym. Lett.* **2010**, *4*, 659.
38. Ahmad, E.; Luyt, A. *Polym. Compos.* **2012**, *33*, 1025.
39. Qian, S.; Wang, H.; Zarei, E.; Sheng, K. *Compos. B Eng.* **2015**, *82*, 23.